ELSEVIER

Deep-Sea Research II 52 (2005) 145–167

DEEP-SEA RESEARCH
PART II

www.elsevier.com/locate/dsr2

Cetacean distributions relative to ocean processes in the northern California Current System

Cynthia T. Tynan[a,*], David G. Ainley[b], John A. Barth[c], Timothy J. Cowles[c], Stephen D. Pierce[c], Larry B. Spear[b]

[a]*Department of Physical Oceanography, Woods Hole Oceanographic Institution, Woods Hole, MA 02543, USA*
[b]*H.T. Harvey and Associates, San Jose, CA 95118, USA*
[c]*College of Oceanic & Atmospheric Sciences, Oregon State University, Corvallis, OR 97331-5503, USA*

Accepted 25 September 2004

Abstract

Associations between cetacean distributions, oceanographic features, and bioacoustic backscatter were examined during two process cruises in the northern California Current System (CCS) during late spring and summer 2000. Line-transect surveys of cetaceans were conducted across the shelf and slope, out to 150 km offshore from Newport, Oregon (44.6°N) to Crescent City, California (41.9°N), in conjunction with multidisciplinary mesoscale and fine-scale surveys of ocean and ecosystem structure. Occurrence patterns (presence/absence) of cetaceans were compared with hydrographic and ecological variables (e.g., sea surface salinity, sea surface temperature, thermocline depth, halocline depth, chlorophyll maximum, distance to the center of the equatorward jet, distance to the shoreward edge of the upwelling front, and acoustic backscatter at 38, 120, 200 and 420 kHz) derived from a towed, undulating array and a bioacoustic system. Using a multiple logistic regression model, 60.2% and 94.4% of the variation in occurrence patterns of humpback whales *Megaptera novaeangliae* during late spring and summer, respectively, were explained. Sea surface temperature, depth, and distance to the alongshore upwelling front were the most important environmental variables during June, when humpbacks occurred over the slope (200–2000 m). During August, when humpbacks concentrated over a submarine bank (Heceta Bank) and off Cape Blanco, sea surface salinity was the most important variable, followed by latitude and depth. Humpbacks did not occur in the lowest salinity water of the Columbia River plume. For harbor porpoise *Phocoena phocoena*, the model explained 79.2% and 70.1% of the variation in their occurrence patterns during June and August, respectively. During spring, latitude, sea surface salinity, and thermocline gradient were the most important predictors. During summer, latitude and distance to the inshore edge of the upwelling front were the most important variables. Typically a coastal species, harbor porpoises extended their distribution farther offshore at Heceta Bank and at Cape Blanco, where they were associated with the higher chlorophyll concentrations in these regions. Pacific white-sided dolphin *Lagenorhynchus obliquidens* was the most numerous small cetacean in early June, but was rare during August. The model explained 44.5% of the variation in their occurrence pattern, which was best described by distance to the upwelling front and acoustic backscatter at 38 kHz. The model of the occurrence

*Corresponding author. Tel.: +1 508 289 3364; fax: +1 508 457 2181.
E-mail address: ctynan@whoi.edu (C.T. Tynan).

0967-0645/$ - see front matter
doi:10.1016/j.dsr2.2004.09.024

pattern of Dall's porpoise *Phocoenoides dalli* was more successful when mesoscale variability in the CCS was higher during summer. Thus, the responses of cetaceans to biophysical features and upwelling processes in the northern CCS were both seasonally and spatially specific. Heceta Bank and associated flow-topography interactions were very important to a cascade of trophic dynamics that ultimately influenced the distribution of foraging cetaceans. The higher productivity associated with upwelling near Cape Blanco also had a strong influence on the distribution of cetaceans.

1. Introduction

The goal of US GLOBEC is to understand and predict how marine species respond to global climate change. Among the uncertainties in a warmer global climate is the extent to which upwelling will increase or decrease in specific boundary current systems, such as the California Current System (CCS), and consequently affect the productivity and structure of marine communities. On decadal scales, climate-related shifts in ecosystem structure of the CCS have been well documented (Roemmich and McGowan, 1995; Mantua et al., 1997; Peterson and Schwing, 2003). The goal of our research, a component of the US GLOBEC Northeast Pacific CCS program (Batchelder et al., 2002; Strub et al., 2002), is to determine how top-trophic predators (i.e., mammals and seabirds) in the northern CCS relate to middle trophic levels and bio-physical coupling in the system. Stemming from these studies, our long-term objective is to develop predictive biophysical models of cetacean occurrence patterns to improve our understanding of the responses of top predators to climate-related variability in the structure of an upwelling boundary current system.

Enhanced productivity associated with coastal upwelling systems can provide important predictable summer foraging for large whales (Fiedler et al., 1998; Gill, 2002). The frequency, duration and seasonal cycle of upwelling in the northern CCS also is expected to have important effects on the productivity and community structure of lower and middle trophic levels, and hence top-trophic levels. During strong upwelling years, euphausiids are the dominant food consumed by many species of pelagic nekton in the CCS (Ainley and Boekelheide, 1990; Brodeur and Pearcy, 1992; Ainley et al., 1996). In central California, Ainley et al. (1996) found that upwelling conditions are favorable to the availability of the euphausiid *Thysanoessa spinifera*, an important prey species for many fish, seabirds and whales. Off southern California, the distribution of *Balaenoptera* whales is determined by their attraction to areas of predictable high densities of *Euphausia pacifica* and *T. spinifera* (Croll et al., 1998). During summer and fall, blue whales *Balaenoptera musculus* are found in cold, well-mixed, productive water that upwells along the coast north of Point Conception and advects south (Fiedler et al., 1998). However, in more northern sections of the west coast of North America, the influence of upwelling and dynamics of the northern CCS on cetaceans have been far less studied. Our GLOBEC study is the first multidisciplinary program in the northern CCS to apply synoptic integrative oceanographic sampling of mesoscale and fine-scale processes to the study of cetacean ecology.

The GLOBEC Northern CCS study region (41.9–44.6°N) occurs within an eastern boundary current system that extends along the west coast of North America from the Strait of Juan de Fuca to the tip of Baja California (Hickey, 1998). Normally, during the spring and summer upwelling season, mean wind stresses are southward, sea levels are low, and sea surface temperature (SST) is cool over the northeast Pacific continental shelf (Strub et al., 1987). When the upwelling index is high, an alongshore, subsurface ribbon of cool water and an equatorward surface jet are usually observed over the shelf (Huyer and Smith, 1974; Smith et al., 1999). On a finer scale, during persistent upwelling, broad tongues and narrow filaments of cold, chlorophyll-rich water may extend over 100 km offshore and downstream, usually associated with coastal promontories (Hood et al., 1990; Barth et al., 2002). The latter applies to Cape Blanco, an important topographic feature in our study region. Here the upwelling jet

separates from the shelf and meanders equatorward as an oceanic jet (Strub et al., 1991; Batteen, 1997; Barth et al., 2000). To examine the ecological importance of the flow-topography interactions at Cape Blanco on productivity, and consequently on cetacean distribution, is among our objectives. In addition, our GLOBEC study was designed to examine the ecological influence of one of the major banks in the CCS (Heceta Bank, 44–44.5°N). We hypothesize that upwelling, flow-topography interactions, and local recirculations associated with the bank generate enhanced seasonal productivity in this region, and that this will attract foraging cetaceans.

2. Materials and methods

2.1. Oceanographic data

Hydrographic data were collected using a towed, undulating vehicle known as 'SeaSoar' (Pollard, 1986), cycled rapidly from the surface to depth while being towed at 3.6 m s^{-1} (7 kts). The vehicle was equipped with a Seabird SBE 911 + conductivity-temperature-depth (CTD) instrument with pumped, dual temperature-conductivity sensors pointing forward through a hole in the SeaSoar nose. A Western Environmental Technology Laboratories (WET Labs) Flashpak fluorometer, using green excitation (490, 30 nm bandpass) and 685-nm detection wavelength, was used to estimate chlorophyll fluorescence. The signal was converted to chlorophyll (mg m^{-3}) using a calibration developed from discrete samples measured with high-performance liquid chromatography. Most CTD-data were collected by cycling SeaSoar on a bare hydrographic cable from the sea surface to 115–120 m over deep water and to within 10 m of the bottom over the shelf. Cycle time in deep water was about 6.5 min. The result was hydrographic data with high spatial resolution (1.3 km between surface points and 500 m between profiles at mid-depth) obtained rapidly (cross-margin sections in 2–10 h and large-area maps in 2–6 days) so that a detailed, synoptic view of the system was available. Over the shallow continental shelf, SeaSoar was cycled from 0–55–0 m every 1.5 min, which resulted in profiles separated by about 300 m at the surface and 170 m at mid-depth. In order to sample to greater depths over the continental slope, SeaSoar also was towed using a faired cable cycling from 0–300–0 m every 8 min. Concurrently, data were logged from a hull-mounted Acoustic Doppler Current Profiler (ADCP). Further details of this hydrographic data set can be found in Barth et al. (2005).

Using time varying lags and an optimized thermal mass correction, the 24-Hz temperature and conductivity data were realigned and corrected to calculate 24-Hz salinity, and averaged to yield 1-Hz values (Barth et al., 2000). The final 1-Hz data files contain unfiltered GPS latitude and longitude; pressure; temperature; salinity; and density anomaly (sigma-*t*, for example as 1024 kg m^{-3} minus 1000) computed using the 1980 equation of state; chlorophyll concentration (mg m^{-3}); date and time. The 1-Hz SeaSoar CTD data were first averaged vertically into 2-dbar bins, from which environmental indices were derived. These included sea surface temperature (SST where surface refers to 5-m depth), sea surface salinity (SSS), thermocline depth, halocline depth, and chlorophyll maximum. The indices were averaged into along-track bins of approximately 15 min (or 4.4 km at average ship speed of 9.5 knots) for comparison with seabird (Ainley et al., 2005) and mammal data.

Acoustic volume backscattering (dB) data were collected with a Hydroacoustics Technology, Incorporated (HTI) model 244 echosounder using frequencies of 38, 120, 200, and 420 kHz. The four transducers were deployed on a towed body at about 4 m depth off the port side of the ship, in combination with the SeaSoar vehicle off the stern. The HTI instrument collected echo integration data in 1 m bins using a raw ping rate of 4 ping s^{-1} or 1 ping s^{-1} for each frequency. These data were averaged into 12-s ensembles, resulting in a horizontal distance of about 50 m between adjacent ensembles. For this study, we use depth-integrated backscatter from the surface to 100 m, and averaged over 15-min segments of trackline, for comparison with seabird and cetacean data. Roughly, the 38 kHz backscatter gives an approximate measure of fish, the 120 and 200 kHz

can be associated with larger and smaller euphausiids respectively, and the 420 kHz is most closely related to copepods. Further discussion of the interpretation of bioacoustic data can be found in Ressler et al. (2005), and references therein.

The spatially averaged temperature, salinity and pressure data were used to compute geopotential anomaly (dynamic height in meters multiplied by the acceleration of gravity) in $J\,kg^{-1}$ ($m^2\,s^{-2}$) relative to 100 db. On east–west sections where SeaSoar profiles were shallower than 100 db, geopotential anomaly was calculated using the extrapolation technique described by Reid and Mantyla (1976). The geopotential anomaly of $2.35\,m^2\,s^{-2}$ is indicative of the center of the equatorward jet and the $2.0\,m^2\,s^{-2}$ marks the inshore side of the jet. Distances to each of these features were included as variables in the analyses. In addition, since the dynamic height reflects the subsurface structure, we also tested distance to a surface feature (i.e. distance to the SST isotherm 11.5 °C during June and 12.0 °C during August) that best represented the inshore side of the alongshore upwelling front.

2.2. Cetacean surveys

Line-transect surveys of cetaceans were conducted during the periods May 29–June 13 and July 27–August 12, 2000 across the shelf and slope off Oregon and northern California (41.9–44.65°N) from the coast to ~125.5°W (Fig. 1). Surveys were conducted in passing mode while the R.V. *New Horizon* was in transit between stations for hydrographic and zooplankton sampling. Surveys were designed to follow 12 mesoscale across-shelf and slope transects and additional fine-scale survey lines similar to those run by a second ship, R.V. *Wecoma*, for acquisition of hydrographic data (see Barth et al., 2005; their Fig. 1). Observations were conducted from the flying bridge during daylight (~0600–2030) whenever sufficient visibility (i.e., ⩾2 nm) and weather (i.e., ⩽Beaufort 6) allowed. Two observers simultaneously surveyed to the horizon with 25×150 binoculars, equipped with compass and reticle. Each observer surveyed a 100° arc from 10° off the bow (opposite side) to 90° on their side of the ship. A third observer focused on the track-line by eye, aided with 7×50 hand-held binoculars. Sightings

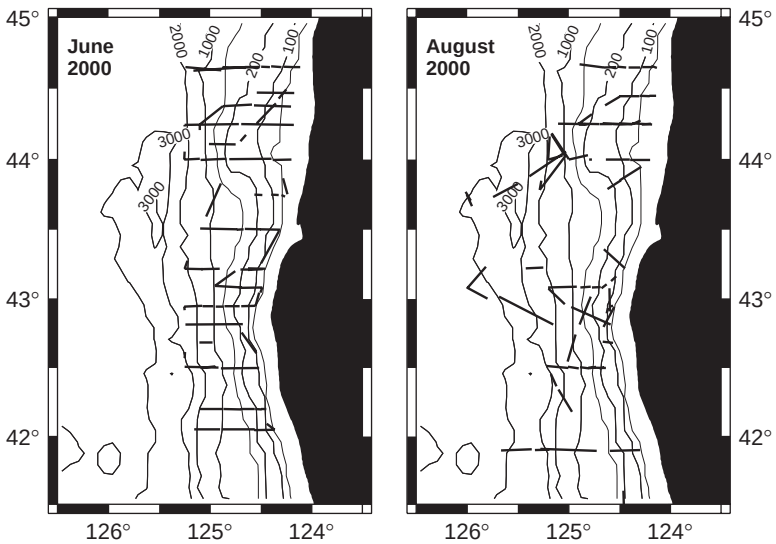

Fig. 1. Cetacean survey effort using 25×150 binoculars (solid bold line segments) during May 29–June 13 and during July 27–August 12, 2000 in the northern California Current System.

were entered immediately on a laptop computer connected to the ship's GPS system. Positions of all sightings were corrected to reflect the actual location of the cetaceans, rather than the ship's position. The height from the surface of the water to the eyes of observers on the 25×150 binoculars was 10.87 m. Under optimal conditions, balaenopterids observed up to 8.0 km from the ship could be identified to species; whales on the horizon (10.4 km) could not be identified to species. Abundance estimation and related methodology will be reported elsewhere.

2.3. Modeling occurrence patterns of cetaceans

Occurrence (presence/absence) patterns of cetaceans relative to ocean processes and biological backscatter were examined for four species having a sufficiently large sample size (i.e. number of sightings obtained while on 25×150 binocular effort): humpback whale *Megaptera novaeangliae*, harbor porpoise *Phocoena phocoena*, Dall's porpoise *Phocoenoides dalli*, and Pacific white-sided dolphin *Lagenorhynchus obliquidens*. Each sighting for these four species was assigned to the nearest 15-min segment of track-line (or approximately 4.4 km at average ship speed of 9.5 kts) for which a suite of 16 hydrographic, acoustic and ecological variables were available (see above). The time difference between the collection of hydrographic data and the acquisition of line-transect survey data was never more than about 12 h, as the two ships were never separated by more than this time lag. The coherence in time and space of the inshore (depth $< \sim 100$ m) and offshore (depth $> \sim 100$ m) circulation structures are typically greater than the distances between cetaceans and the track-line (Barth et al., 2005). For example, the offshore meanders are long-lived and last for weeks to months. Inshore, currents throughout the water column and surface temperature and salinity change with the wind forcing on a time scale 2–10 days. The deeper ($\sim$50 m) horizontal density, temperature and salinity fronts are more stable. In general, the alongshore correlation length scales are much longer than the cross-shelf correlation length scales. Kundu and Allen (1976), using moored velocity data, found alongshore and cross-shelf correlation scales of at least 30 km (i.e. about the same size as our distances between mesoscale survey lines, and significantly larger than the distances of cetacean sightings to the track-line and the nearest grid segment of SeaSoar-derived environmental data).

Multiple logistic regression was used to model cetacean occurrence (Cox and Snell, 1989), because outcomes were treated as binary (a cetacean species was either present or absent within a 15-min transect). An important assumption of logistic regression is that outcomes are binomially distributed (Cox and Snell, 1989); therefore, we confirmed that occurrence of each species did not deviate from binomial distribution (goodness of fit X^2-test, $P > 0.05$). We also tested for autocorrelation of cetacean occurrence among the 15-min transect segments for each species using (the 'acf' command of) S-PLUS (S-PLUS, 1997). Occurrence patterns were not autocorrelated among transects for any of the species.

Maximum-likelihood logistic regression was implemented using program STATA (STATA Corporation, 1995); the 'logit' command for the likelihood ratio test was used to examine the occurrence of each species by season (i.e. May–June and July–August) relative to two spatially fixed variables (latitude, depth) and the following 14 spatially varying variables: SST, SSS, depth of the thermocline, thermocline gradient, depth of the halocline, halocline gradient, distance to the jet 'center' (geopotential anomaly of $2.35\,m^2\,s^{-2}$), distance to the inshore edge of the jet (geopotential anomaly of $2.0\,m^2\,s^{-2}$), distance to the inshore edge of the surface front (11.5 °C SST isotherm during spring and 12.0 °C SST isotherm during summer), value of chlorophyll *a* maximum, and integrated acoustic backscatter at four frequencies (38, 120, 200, and 420 kHz). A total of 420 grid-segments, for which cetacean effort (while on 25×150 binoculars) and the full suite of SeaSoar-derived and bioacoustic data were available, were used in the multiple logistic regression models: 226 segments in May–June and 194 segments in July–August (Fig. 2). We report the likelihood ratio statistic, which is equivalent to 'deviance' as reported in generalized linear models, and therefore is analogous to sums of squares reported in

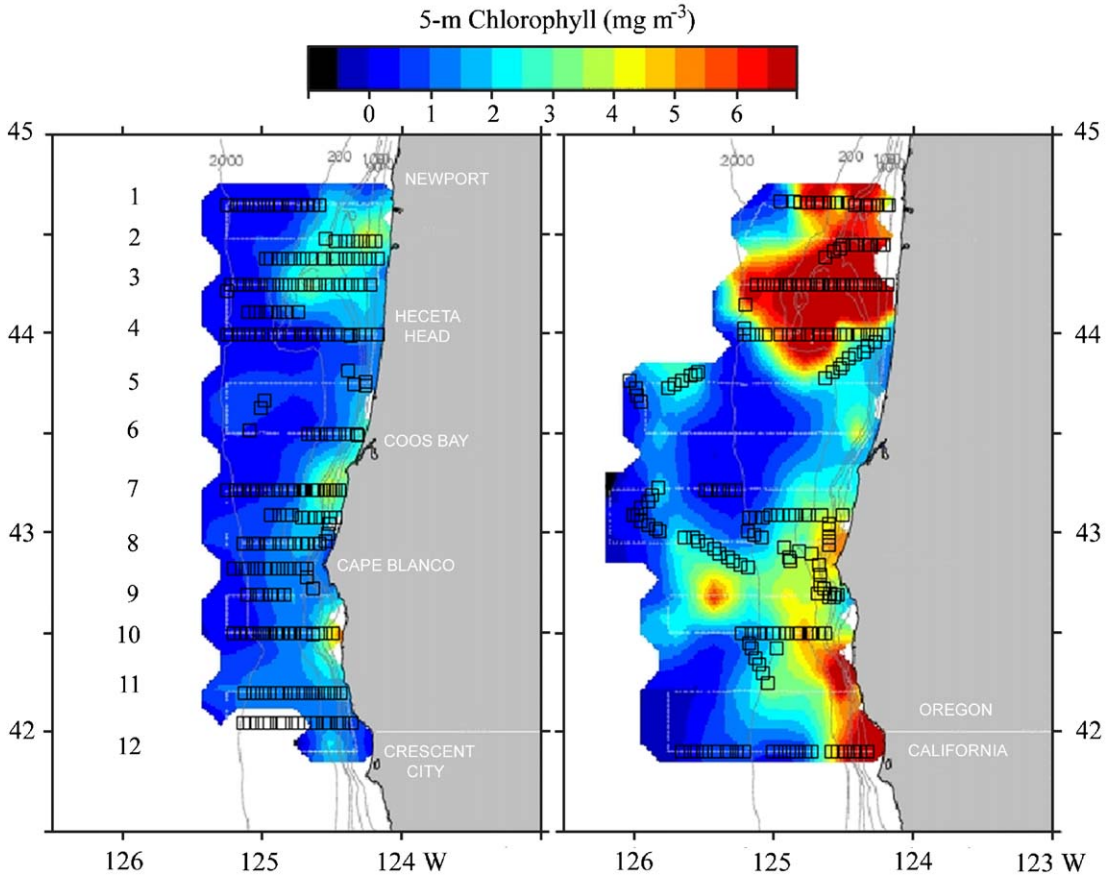

Fig. 2. Location of the starting position for each 15-min survey segment (square) used in the multiple logistic regression models of cetacean occurrence, May–June and July–August 2000, relative to chlorophyll *a* concentration at 5 m. All segments used in the models had coverage of line-transect survey effort for cetaceans, oceanographic sampling using the towed SeaSoar vehicle, and bioacoustic sampling using the multi-frequency system.

ANOVA. We evaluated departure from linearity by testing whether the coefficients of a polynomial logistic regression model (to order 2) differed significantly from zero.

We modeled occurrence patterns for each species by season, except for Pacific white-sided dolphin. The number of sightings (3) of Pacific white-sided dolphins during August 2000 was insufficient for meaningful analysis; therefore, we modeled occurrence pattern for this species after combining spring and summer data. To control for possible diurnal patterns in cetacean behavior or migratory activity during the cruise period, we included time of day and Julian date in the analyses. In addition, wind speed was included in an initial model to check for possible effects of occurrence pattern related to either animal activity during increased sea state or reduced probability of detection with increased sea state. Wind speed was insignificant for 5 of the 7 models (humpback whales in both seasons, Dall's porpoise in both seasons, and harbor porpoise in spring) and adding wind speed reduced the explained variance in every model (except for a slight improvement in the model of Pacific white-sided dolphin). Therefore, to develop the best predictive models and to test the direct effects of ocean conditions resulting from wind-driven upwelling, wind speed was not included in the final models.

The multiple logistic regression analyses were conducted by initially entering all 16 independent variables together in each model. Using a stepwise procedure, insignificant terms were dropped, one at a time, in order of increasing *P*-values. Because many terms were correlated (Table 2), importance of some variables was likely masked by others in the initial model. Therefore, we tested for effects of eliminated terms by putting them, one at a time, back in the model. The model was complete when no terms could be added or dropped. In a multiple regression model, any independent variables that test as having a significant relationship with the dependent variable (cetacean occurrence) are true influences (Seber, 1977; Kleinbaum et al., 1988). That is, their effects are independent of those of other independent variables (correlated or not) that also have significant relationships with occurrence, because each independent term included in the model is evaluated while taking into account (controlling for) the effect of each of the other independent variables (see Ainley et al., 2005, for additional detail on the properties and benefits of multiple regression analyses when applied to correlated variables).

3. Results

3.1. Correlations among physical and biological oceanographic variables

The physical and biological environmental variables were correlated with one another in 99 (73%) of the 136 possible correlations (Table 1). Considering the relationships having *r*-values >0.4, ($P<0.0001$), for reasons of brevity, the following was indicated: (1) distance to the center of the equatorward jet, sea surface salinity, and abundance of smaller prey (represented by >120 kHz backscatter) increased with Julian date, while density of larger prey (38 kHz size range)

Table 1
The Pearson linear correlation coefficients (*r*) among physical and biological environmental variables[a]; $n = 420$ survey transects, upwelling period 2000

	JD	LT	FRT	JTI	JTC	DPT	SST	SSS	TDP	TST	HDP	HST	CM	38 kHz	120 kHz	200 kHz
LT	0.03															
FRT	0.04	−0.11														
JTI	**0.18**	0.04	**0.80**													
JTC	**0.57**	−0.03	**0.33**	**0.41**												
DPT	**0.23**	**−0.31**	**0.66**	**0.72**	**0.21**											
SST	−0.07	**−0.25**	**0.49**	**0.44**	**−0.21**	**0.58**										
SSS	**0.70**	**−0.23**	−0.09	−0.04	**0.57**	−0.01	**−0.43**									
T-DP	**−0.29**	**−0.24**	**0.40**	**0.33**	**−0.15**	**0.31**	**0.43**	**−0.23**								
T-ST	0.04	−0.06	**0.29**	**0.25**	**−0.23**	**0.36**	**0.78**	**−0.34**	**0.20**							
H-DP	−0.05	**−0.28**	**0.33**	**0.27**	0.06	**−0.34**	**0.37**	−0.02	**0.61**	**0.20**						
H-ST	**−0.71**	0.05	−0.06	**−0.14**	**−0.49**	−0.13	**0.24**	**−0.77**	0.10	**0.26**	0.01					
CM	**0.33**	0.07	**−0.21**	**−0.17**	**0.38**	**−0.31**	**−0.32**	**0.40**	**−0.30**	**−0.19**	**−0.23**	**−0.25**				
38 kHz	**−0.55**	**−0.22**	**0.20**	0.05	**−0.32**	**0.17**	**0.28**	**−0.43**	**0.25**	**0.18**	0.11	**0.38**	**−0.25**			
120 kHz	**0.40**	0.00	**0.21**	**0.25**	**0.19**	**0.37**	**0.20**	0.14	−0.07	**0.21**	0.00	**−0.28**	0.07	**0.38**		
200 kHz	**0.57**	**0.20**	0.14	**0.33**	**0.34**	**0.35**	0.05	**0.25**	**−0.15**	**0.16**	−0.04	**−0.37**	0.13	−0.03	**0.74**	
420 kHz	**0.47**	0.08	**0.30**	**0.37**	**0.34**	**0.43**	**0.15**	0.14	**−0.15**	**0.16**	−0.05	**−0.27**	0.00	−0.02	**0.68**	**0.72**

[a]Relationships having *r*-values in bold were significantly correlated ($P<0.05$). LT, latitude; JD, Julian date; FRT, distance to upwelling surface front defined by 11.5 °C surface isotherm during June and 12.0 °C surface isotherm during August; JTI, distance to the inshore edge of the jet (geopotential anomaly of 2.0 $m^2 s^{-2}$); JTC, distance to the jet 'center' (geopotential anomaly of 2.35 $m^2 s^{-2}$); DPT, ocean depth; SST, sea surface temperature; SSS, sea surface salinity; TDP, thermocline depth; TST, thermocline strength; HDP, halocline depth; HST, halocline strength; CM, value of chlorophyll maximum; 38 kHz, integrated backscatter 0–100 m; 120 kHz backscatter; 200 kHz backscatter; and 420 kHz backscatter. A positive correlation between acoustic backscatter and another variable indicates a positive relationship, and the reverse for a negative correlation.

decreased with date: (2) SST and ocean depth increased with increase in distance between SST-defined shoreward edge of upwelling front and dynamic height defined shoreward edge of jet (the latter also were highly correlated); (3) SSS increased and halocline strength decreased with increase in distance from the center of the equatorward jet; (4) SST and density of the smallest prey size class increased with increase in ocean depth; (5) thermocline depth and gradient increased, while SSS decreased, with increase in SST; (6) value of the chlorophyll maximum increased, halocline strength and abundance of larger prey (38 kHz) decreased with increase in SSS; (7) halocline depth increased with increase in thermocline depth; (8) backscatter at the three highest frequencies increased in accord with one another.

3.2. Cetacean species composition

During August, the cetacean survey coverage was less uniform across the shelf at 43.5°N than during June, in order that the biophysical structure on the outside of a warm mesoscale eddy also could be studied (Fig. 1). Survey coverage extended west over the basin to 126°W to reach the outside of this feature. A total of 223 sightings of cetaceans (1698 animals) were recorded during spring and 298 sightings (614 animals) were recorded during summer (Table 2). Sixteen cetacean species were recorded in the northern CCS during 2000 (Table 2): four species of large whale (humpback *M. novaeangliae*, gray *Eschrichtius robustus*, fin *Balaenoptera physalus*, and sperm whale *Physeter macrocephalus*); seven species of medium-sized whale (minke *Balaenoptera acutorostrata*, killer whale *Orcinus orca*, Baird's beaked whale *Berardius bairdii*, Cuvier's beaked whale *Ziphius cavirostris*, *Mesoplodon* sp., *Hyperoodon* sp., and Risso's dolphin *Grampus griseus*,), and five species of small cetacean (Pacific white-sided dolphin *L. obliquidens*, northern right whale dolphin *Lissodelphis borealis*, Dall's porpoise *P. dalli*, harbor porpoise *Phocoena phocoena*, and dwarf sperm whale *Kogia simus*).

3.3. Occurrence patterns of cetaceans

The multiple logistic regression models explained 25.6–94.4% of the variance in the

Table 2
Summary of cetacean sightings and numbers of animals observed during line-transect surveys conducted in conjunction with two GLOBEC Northeast Pacific Northern California Current cruises during 2000

	Survey 1: May 29–June 13		Survey 2: July 27–August 13	
Species	# Sightings	# Animals	# Sightings	# Animals
Pacific white-sided dolphin	86	1063	3	40
Dall's porpoise	31	99	130	294
Humpback whale	35	70	45	76
Harbor porpoise	41	62	87	125
Northern right whale dolphin	9	195	0	0
Risso's dolphin	7	87	3	17
Killer whale	4	19	2	9
Sperm whale	2	6	3	3
Baird's beaked whale	5	27	3	13
Mesoplodon sp.	0	0	4	6
Cuvier's beaked whale	0	0	1	1
Hyperoodon sp.	0	0	1	3
Gray whale	1	1	6	14
Fin whale	0	0	6	9
Minke whale	1	1	4	4
K. simus	1	1	0	0

Table 3
Results of multiple logistic regression models to examine occurrence patterns of Pacific white-sided dolphin (PWSD), humpback whale (HBW), Dall's porpoise (DAPO) and harbor porpoise (HAPO) relative to physical and biological oceanographic variables during spring (late May–early June) and summer (late July–early August) 2000

	PWSD	HBWspr	HBWsum	DAPOspr	DAPOsum	HAPOspr	HAPOsum
% Variation explained	44.5	60.2	94.4	25.6	46.1	79.2	70.1
Latitude			$-^{2}$			$+^{1}$	$+^{1}$
Distance to Front A	−	$-^{3}$	−		M	+	$-^{2}$
Distance to 2.0 $m^2 s^{-2}$	M^{1}	+	+		$-^{2}$	−	
Distance to 2.35 $m^2 s^{-2}$		−	−			−	$+^{3}$
Ocean depth	+	$+^{2}$	$-^{3}$		$+^{1}$	−	
SST		$+^{1}$	−		M	+	
SSS	−	M	M^{1}			$+^{2}$	
Thermocline Depth		−			−	+	
Thermocline Gradient						M^{3}	
Halocline depth						−	
Halocline gradient						M	−
Backscatter 38 kHz	$^{A}+^{2}$	$^{C}+$	$^{B}+$		$^{A}+^{3}$		
120 kHz	$^{B}-^{3}$		^{C}M			−	$^{A}+$
200 kHz		$^{B}+$	M	$^{B}-^{2}$		^{C}M	$^{B}-$
420 kHz				$^{A}+^{1}$		$^{A}+$	^{C}M
Chlorophyll maximum	$^{C}-$	$^{A}+$	$^{A}+$			$^{B}+$	

Shown are the signs of the regression coefficients for variables significantly related to occurrence: (+), positive response to increase in a variable; (−), negative response; and "M", curvilinear response where a significant linear effect was not observed. Superscripts (1, 2, and 3) adjacent to a coefficient indicate that the variable explained the first, second, or third largest amount of variance in a species' occurrence; superscripts (A, B, and C) indicate that the variable explained the first, second, or third largest amount of variance among the five biological variables (acoustic backscatter at four frequencies, and value of chlorophyll *a* maximum). Details of the variables are presented in the methods section: distance to the jet 'center' (geopotential anomaly of 2.35 $m^2 s^{-2}$); distance to the inshore edge of the jet (geopotential anomaly of 2.0 $m^2 s^{-2}$); and distance to inshore surface expression of upwelling front (11.5 °C SST isotherm during June and 12.0 °C SST isotherm during August). The latter surface front is referred to as Front A above. A negative coefficient for distance to an ocean feature indicates that the species occurred near the feature. A positive coefficient for cetacean response to backscatter indicates that the species occurred more frequently at higher densities of the plankton or nekton described acoustically by that backscatter.

distributions of four cetacean species by season (Table 3). The number of variables significantly related to occurrence pattern ranged from two (of the possible 16 variables) for Dall's porpoise (spring) to 15 significant variables for harbor porpoise (summer). The variable most often significantly related to occurrence pattern was the distance to the inshore edge of the upwelling front (SST-defined). This variable was significant in six of the seven models (Table 3). Other important variables that were significant in four or five models included: distance to the inshore edge of the jet, distance to the center of the jet, ocean depth, sea surface salinity, acoustic backscatter at three frequencies (38, 120 and 200 kHz), and value of the chlorophyll maximum.

3.3.1. *Humpback whale*

The humpback whale was the most abundant large cetacean during late spring and summer (Table 2), although, their distribution varied greatly with season (Fig. 3). Spatially, humpback whales exhibited a bimodal cross-shelf distribution in spring. Some humpbacks occurred in cold, saline, upwelled waters of higher surface chlorophyll north and south of Cape Blanco (Fig. 2). Most humpbacks, however, remained over the slope (200–2000 m) in warmer SSTs (>12 °C) and

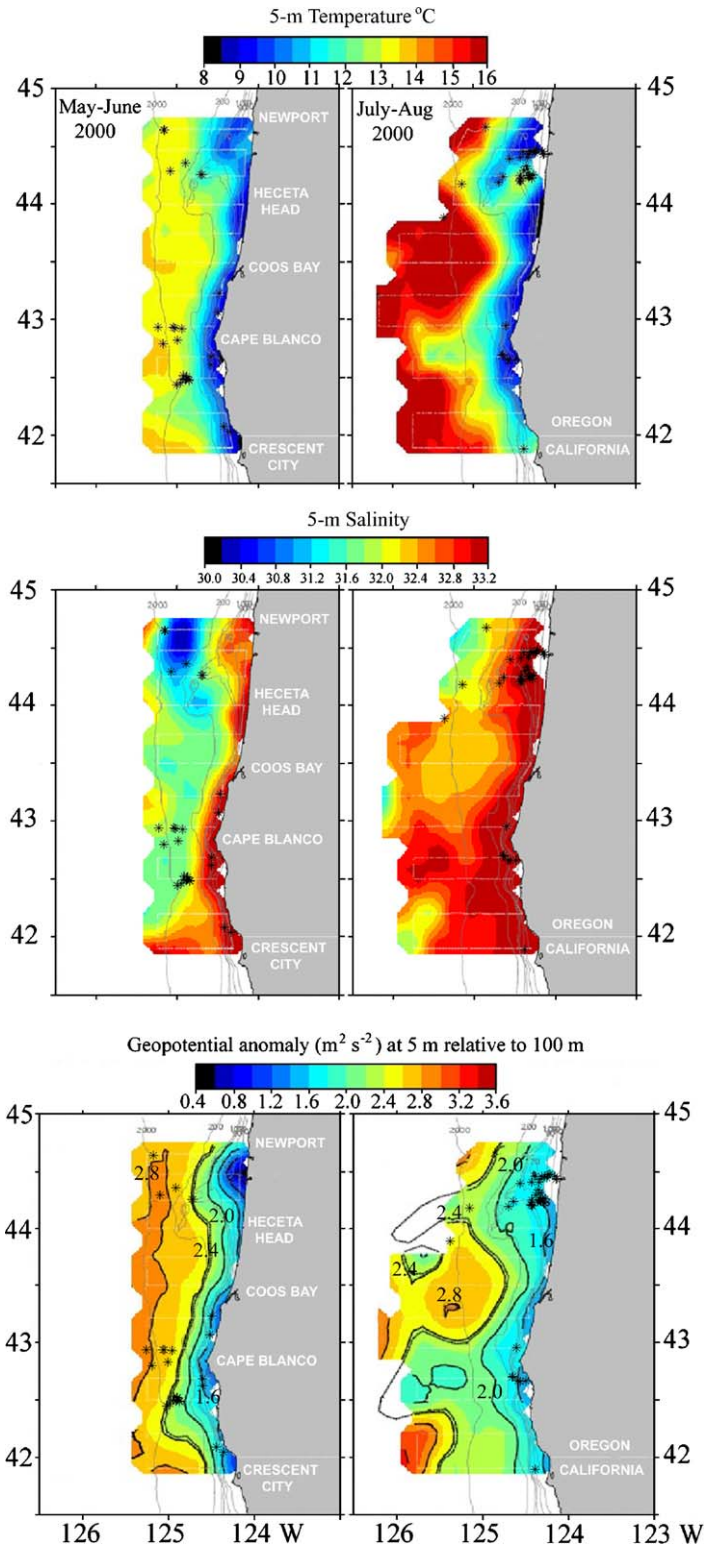
5-m Temperature °C
8 9 10 11 12 13 14 15 16
May-June 2000
July-Aug 2000
NEWPORT
HECETA HEAD
COOS BAY
CAPE BLANCO
CRESCENT CITY
OREGON
CALIFORNIA
45
44
43
42
5-m Salinity
30.0 30.4 30.8 31.2 31.6 32.0 32.4 32.8 33.2
Geopotential anomaly (m² s⁻²) at 5 m relative to 100 m
0.4 0.8 1.2 1.6 2.0 2.4 2.8 3.2 3.6
126 125 124 W
126 125 124 123 W

intermediate surface salinities (Fig. 3). A multiple logistic regression model explained 60.2% of the variance in their distribution pattern during spring (Table 3). Humpback distribution was most correlated with sea surface temperature, depth, and distance to the surface expression of the upwelling front (i.e. whales were near the 11.5 °C surface isotherm). In addition, humpback occurrence was significantly negatively correlated with distance to the 'jet' center (i.e. whales over the slope are near the geopotential anomaly 2.35 $m^s s^{-2}$) and thermocline depth (i.e. whales were associated with shallower mixed layer) (Table 3). Humpback occurrence was significantly positively correlated with distance to the shoreward edge of the jet (i.e. whales were farther from the geopotential anomaly 2.0 $m^s s^{-2}$), integrated backscatter at 38 kHz (i.e. larger acoustic targets such as fish) and 200 kHz (i.e. zooplankton such as euphausiids), as well as the value of the chlorophyll maximum (Table 3). Of the latter three biological variables, value of the chlorophyll maximum was most strongly correlated with humpback occurrence. During spring, humpback occurrence had a significant curvilinear (nonlinear) relationship to surface salinity. Humpback whales did not occur in the lowest salinity water (<30.8) of the Columbia River plume (Fig. 3).

The multiple logistic regression model of humpback whale distribution during August explained 94.4% of the variance in occurrence pattern (Table 3). Surface salinity was the most significant variable, followed by latitude and depth. As was the case in spring, humpback occurrence during summer had a significant curvilinear (nonlinear) relationship to surface salinity, and humpbacks appear to avoid the low-salinity surface plume offshore (Fig. 3). The negative correlation with both distance to the inshore edge of the surface front (11.5 °C isotherm) and distance to the jet center reflect the bimodal distribution of humpbacks in the northern region (~44°N) (Table 3 and Fig. 3). Although most humpbacks occurred on the shelf near the shoreward edge of the upwelling front, a few whales occurred on the slope associated with the strong mesoscale variability in the jet. The seasonal shift in humpback distribution to the broad shelf at Heceta Bank (44–44.5 °N) is reflected in the significant negative correlation with depth. Humpback whales on the shelf typically occurred in depths <100 m on Heceta Bank and off Cape Blanco (Fig. 3). Of the biological variables tested in the model, value of the chlorophyll maximum was most strongly correlated with humpback occurrence, followed by integrated backscatter at 38 kHz (Table 3 and Fig. 4). Humpback whales occurred in upwelled waters on Heceta Bank and off Cape Blanco, associated with higher surface chlorophyll, higher integrated backscatter at 38 kHz and high densities of juvenile salmon (Fig. 5). On Heceta Bank, humpbacks occurred within a zone of lower mean near-surface velocities and recirculation (see ADCP-derived velocity vectors at 5 m, Fig. 6).

3.3.2. Other balaenopterids

Fin whales were only found during August, when survey effort extended further offshore (~126°W; >2000 m) to the western edge of an anticyclonic mesoscale eddy or meander (43.75°N) (Fig. 6). Fin whales occurred in the surface flow of higher chlorophyll that was advected northward on the western side of the meander (see surface chlorophyll, Fig. 4). Fin whales appear to prefer the outer, basin region of influence of the coastal jet. Therefore, during summer, fin whales and humpback whales are widely separated in the northern CCS. Gray whales were observed very close to the coast in cold (<9.5° C) upwelled waters, especially near Cape Blanco in August

Fig. 3. The correspondence of humpback whale sightings (*) with sea surface (5 m) temperature, surface salinity, and geopotential anomaly at 5 m relative to 100 m, during May–June and July–August, 2000. Several features related to upwelling were included in the models of cetacean occurrence: the center of the equatorward jet, defined by geopotential anomaly 2.35 $m^2 s^{-2}$ (the double heavy line); the shoreward edge of the jet, defined by geopotential anomaly 2.0 $m^2 s^{-2}$ (first single heavy line inshore of the jet center); and the shoreward edge of the surface front in SST, defined by the 11.5 °C isotherm (blue-to-green boundary) during June and the 12.0 °C isotherm during August. The stars (*) mark the location (occurrence) of humpback whales sightings and do not reflect the number of whales in each sighting.

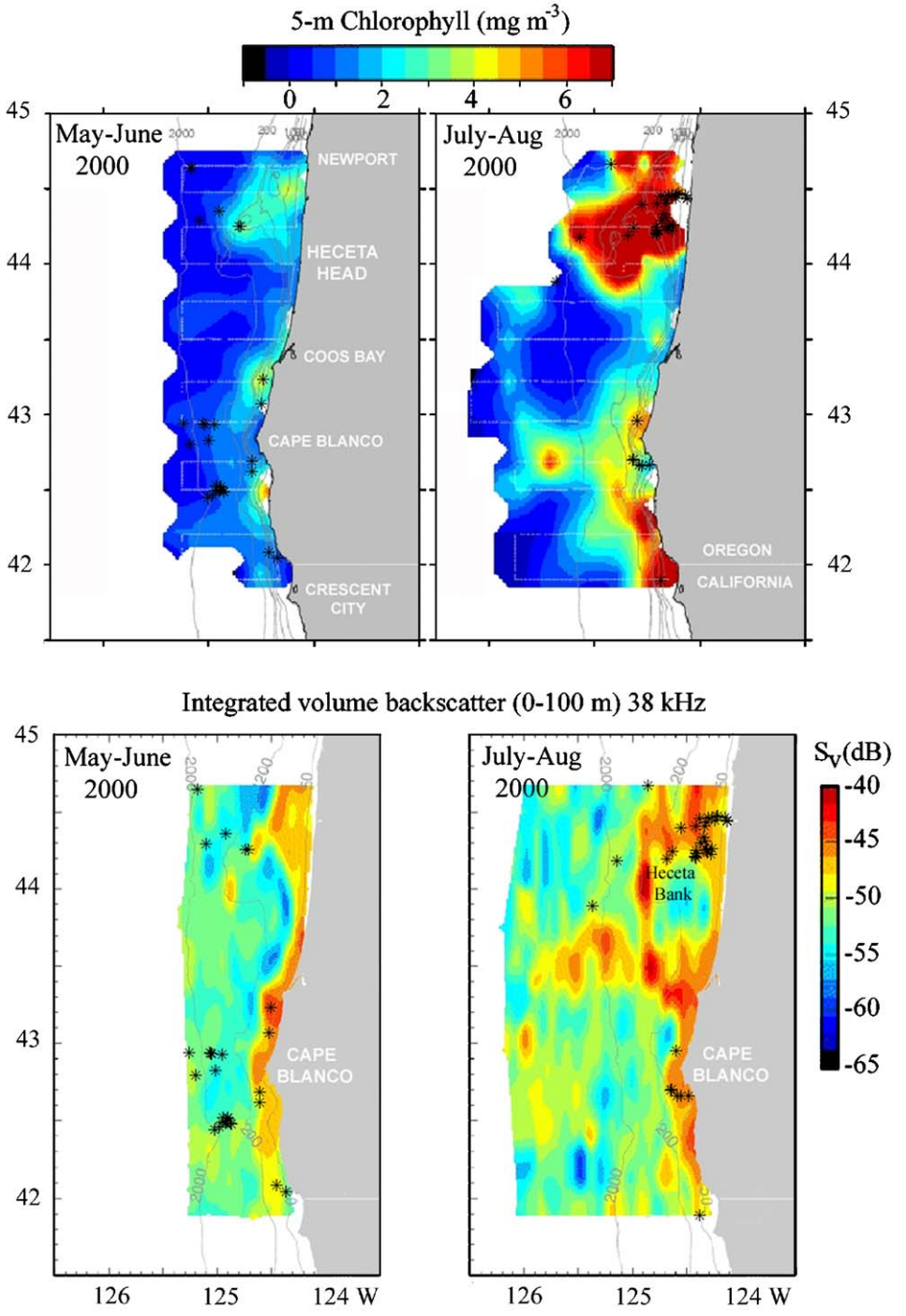

Fig. 4. The correspondence of humpback whale sightings (*) with surface (5 m) chlorophyll and volume acoustic backscatter at 38 kHz integrated over 0–100 m, during May–June and July–August 2000. A higher (less negative) value of integrated backscatter (dB) indicates greater scattering at that frequency. The correspondence between humpback whales and higher chlorophyll and higher backscatter at 38 kHz is evident near Cape Blanco during spring and on Heceta Bank during summer.

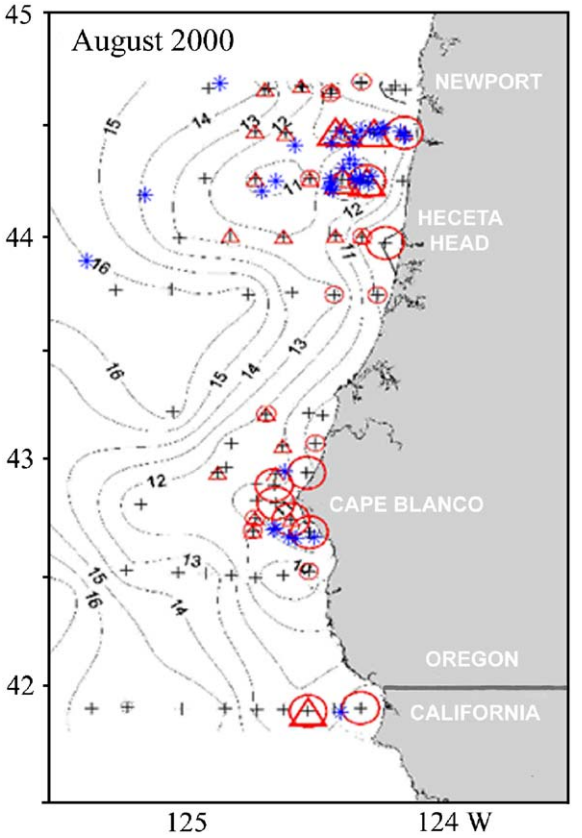

Fig. 5. The correspondence of humpback whale sightings (blue stars) overlaid on catch distribution for juvenile coho *Oncorhynchus kisutch* (red triangles) and chinook salmon *O. tshawytscha* (red circles) from surface trawls (Brodeur et al., 2004) conducted during August 2000. Catch data is overlaid on surface temperature contours. The size of the triangles and circles is proportional to the size of the catch: smaller symbols represent catch of 1–5 salmon; larger symbols represent catch of 6–150 salmon. Plus signs are stations sampled where no salmon were caught. The correspondence between humpback whales and regions of higher juvenile salmon abundance (near Heceta Bank and off Cape Blanco) is clear.

(Fig. 6). Though minke whales were observed on the shelf, they were very rare.

3.3.3. Large odontocetes

There is some suggestion that the broader slope at 43–43.5°N is less important to deep-diving odontocetes (or their prey) than the steep bathymetry along a submarine bank, Heceta Bank, and the slope off and south of Cape Blanco (Fig. 6). Of the deep-diving large odontocetes, Baird's beaked whale was sighted most frequently (Table 1) and occurred at water depths >1000 m on the slope (Fig. 6). Sperm whales were only sighted in slope waters west or southwest of Heceta Bank, where the bathymetry is steep and the coastal jet is strongly influenced by the bottom topography (Figs. 3 and 6). During August, four species of deep-diving large odontocetes (i.e. sperm whale, Baird's beaked whale, Cuvier's beaked whale, and *Mesoplodon* sp.) occurred west and southwest of the submarine bank, in a band of surface (5-m) convergence between the equatorward flowing jet and the northward flow along the edge of an anticyclonic mesoscale eddy or meander (Fig. 6). Though velocities were uniformly southward in the upper 150 m during June, during August the velocity structure in this region was complex with flow reversals (northward versus southward) in both the vertical and across-shelf structure (see velocity structure at Line 3, 44.24°N; Barth et al., 2005 their Fig. 9).

3.4. Mesoscale distributions of dolphins and porpoises

Pacific white-sided dolphin was the dominant small cetacean over the slope (200–2000 m) during June; however, by August this species was rare in the study region (Table 1, Fig. 7). Results of the multiple logistic regression model explained 44.5% of the occurrence pattern of Pacific white-sided dolphins (Table 3). A curvilinear response to distance to the shoreward edge of the jet (geopotential anomaly 2.0 $m^2 s^{-2}$) was the best predictor of the occurrence pattern of this species. The curvilinear effect likely reflects the proximity of Pacific white-sided dolphins to the upwelling front in the southern region and their increased distance from this feature in the northern region (Fig. 7). Near Cape Blanco the upwelling front and center of the jet extend farther offshore over the slope, whereas in the northern area these features are restricted to the shelf during June (Fig. 7). Pacific white-sided dolphins occurred typically to the west of the jet center in the north, but were in the jet in the southern region. The second most important

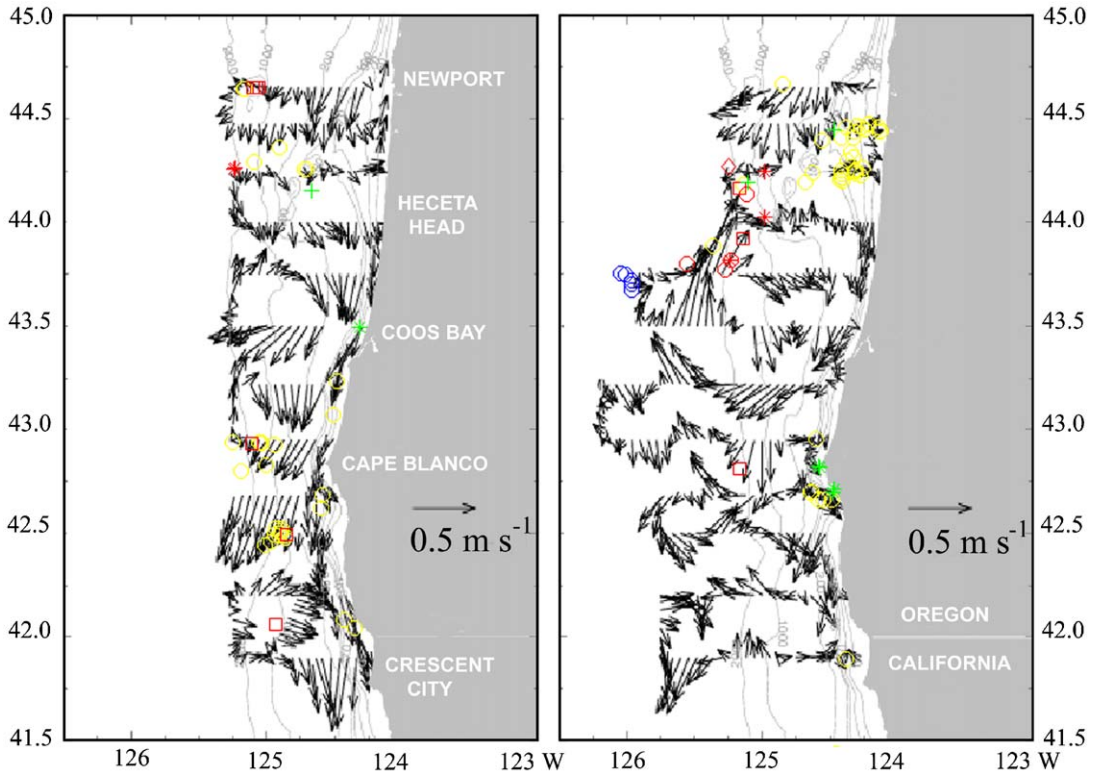

Fig. 6. The distributions of sightings of large cetaceans during May–June and July–August 2000 relative to velocity at 5 m as measured by shipboard Acoustic Doppler Current Profiler. A scale arrow for velocity appears at right. Symbols for each species are as follows: humpback whale (yellow ○); fin whale (blue ○); minke whale (yellow +); sperm whale (red *); Baird's beaked whale (red □); Cuvier's beaked whale (red ◇); *Mesoplodon* sp. (red ○); and gray whale (green *). During August, the higher density of deep-diving odontocetes (red symbols) over the slope in a region of surface convergence between the equatorward jet and the northward flow along the western edge of an anticyclonic mesoscale eddy, is evident.

variable, and also the most important biological variable to explain dolphin occurrence, was integrated acoustic backscatter at 38 kHz (i.e. larger targets such as fish). The occurrence pattern of Pacific white-sided dolphins was also significantly positively correlated with depth and negatively associated with surface salinity (Table 2), reflecting their association with the slope and the lower salinities occurring there due to the influence of the Columbia River water in spring (Fig. 7). Pacific white-sided dolphins occurred around the edges of the low-salinity plume in the northern region (~44.0–44.6°N).

Northern right whale dolphins were often associated with schools of Pacific white-sided dolphins during June. Though the number of sightings was insufficient to use in a model of occurrence pattern, their distribution on the slope was similar to that of Pacific white-sided dolphins. This species was not observed in the study region during the July–August survey. Risso's dolphins (grampus) appeared to be more widely distributed and more abundant in June than in August in the northern CCS off Oregon (Table 2). They occurred in the jet of higher velocity and the upwelling front over the slope off Cape Blanco and over the shelf and slope between 44.0–44.75°N during June. Though often associated with warmer ocean temperatures, this species occurred in SSTs ranging from 10–13 °C during June. Their distribution

during June and August suggests a preference for the slope and outer shelf associated with the submarine bank, Heceta Bank (44.0–44.5°N).

The multiple logistic regression model for Dall's porpoise explained 25.6% of the variance in their distribution during spring, when they were relatively evenly distributed on the slope and occasionally occurred on the shelf at depths >100 m (Fig. 7). Acoustic backscatter at 420 kHz (e.g., smaller plankton such as copepods) was the most important variable to explain this species' distribution during late May and early June (Table 3). There were no significant correlations between Dall's porpoise occurrence and physical variables during spring. However, during summer when mesoscale variability in the CCS was higher, the model was more successful and explained 46.1% of the variance in occurrence pattern (Table 3). Depth and distance to the shoreward edge of the upwelling front (i.e. geopotential anomaly of $2.0\,m^2\,s^{-2}$) were the first and second most important variables to explain the variance in their distribution during summer. Then, the presence of a warm, low-chlorophyll, mesoscale anticyclonic eddy or meander appears to have displaced or concentrated Dall's porpoises to the north and south edges of the meander (Fig. 7). In addition, Dall's porpoise were significantly negatively correlated with thermocline depth, reflecting the shoaling of isotherms at the edges of the warm meander. Their response to SST was curvilinear, as Dall's porpoise occurred in a frontal zone of intermediate SST (12–14 °C) between the warmest offshore water and coolest upwelled water (Fig. 7). During summer, Dall's porpoise occurrence was also significantly positively associated with acoustic backscatter at 38 kHz (i.e. larger prey such as fish), which was the most important biological variable in the model (Table 3).

Harbor porpoise was the dominant small cetacean on the shelf in both seasons (Table 2). Typically a coastal denizen, they were distributed further offshore (out to the ~200 m isobath) on the broad shelf at Heceta Bank and also off Cape Blanco where the jet and upwelling front extend westward (Fig. 8). The mesoscale pattern of harbor porpoise distribution suggests that the narrow shelf region between these features (i.e. south of Heceta Bank and north of Coos Bay, ~43.5–44.0°N) supports fewer harbor porpoises (Fig. 8). The multiple logistic regression model explained 79.2% and 70.1% of the variance in occurrence pattern of harbor porpoises in spring and summer, respectively (Table 3). Their association with the broader shelf or bank in the north makes latitude the most important predictive variable within the study region in both seasons. During spring, surface salinity was the second most important predictive variable to explain the variance in harbor porpoise occurrence. Harbor porpoises occurred in the upwelled water of higher salinity near the coast. Harbor porpoise occurrence was also significantly negatively correlated with distances to the shoreward edge of the upwelling front (i.e. geopotential anomaly $2.0\,m^2\,s^{-2}$) and the center of the jet (i.e. geopotential anomaly $2.35\,m^2\,s^{-2}$), meaning that harbor porpoise were near these features (Table 3 and Fig. 8).

During summer, when the upwelling front and jet occur farther offshore, harbor porpoises are significantly negatively associated with only the distance to the shoreward edge of the surface front (i.e. 12.0 °C SST isotherm) and are significantly positively associated with the jet center (i.e., harbor porpoises are far from the center of the jet) (Table 3 and Fig. 8). Harbor porpoises were associated with regions of higher surface chlorophyll over Heceta Bank and near Cape Blanco in both seasons (Fig. 8), although a significant positive correlation with value of the chlorophyll maximum only occurred during spring (Table 3). Acoustic backscatter at 420 kHz (i.e. small zooplankton such as copepods) and value of the chlorophyll maximum were the first and second most important biological variables, respectively, to explain the variance in harbor porpoise occurrence. During August, harbor porpoise occurrence was significantly correlated with acoustic backscatter at three frequencies (i.e. 120, 200 and 420 kHz); however, only the correlation with 120 kHz, which was the strongest biological variable, was positive (i.e. harbor porpoise occurrence was related to higher backscatter at 120 kHz).

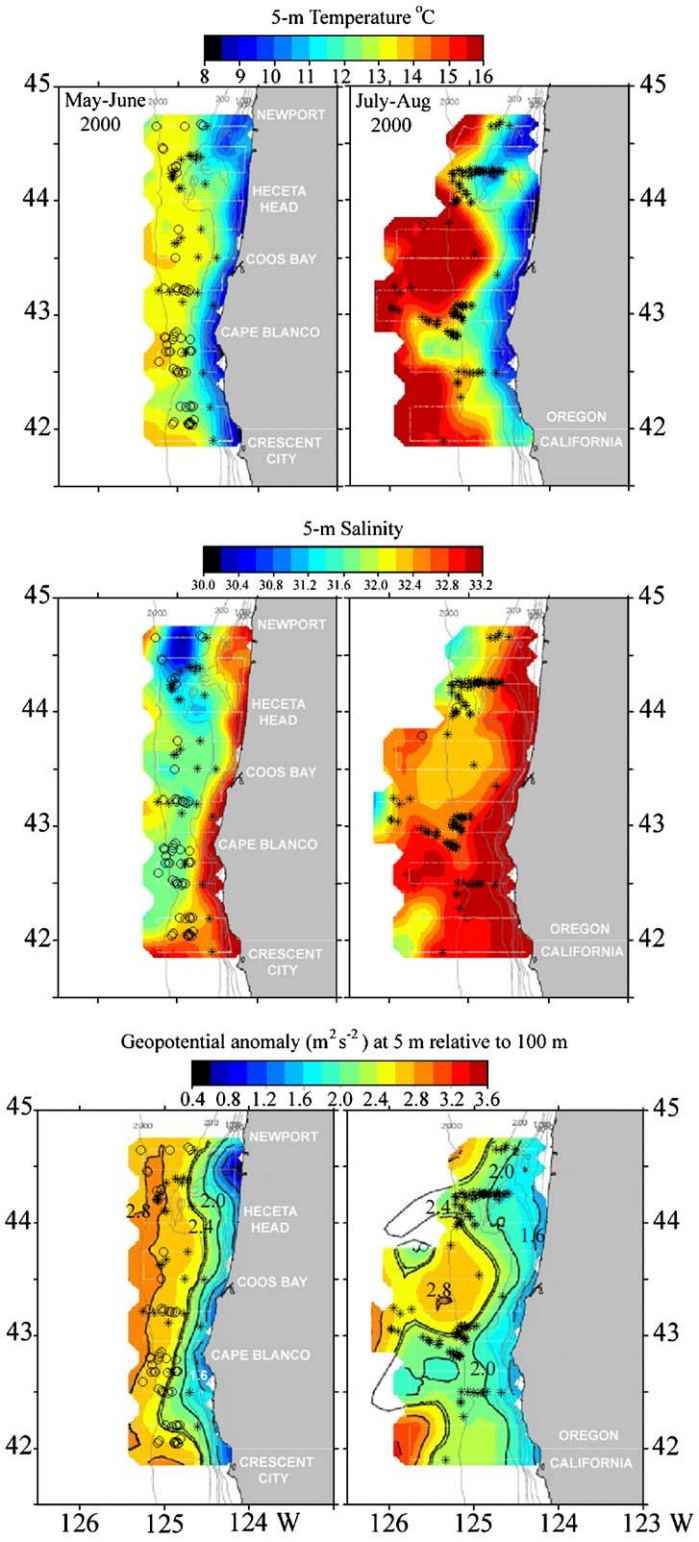
5-m Temperature °C
8 9 10 11 12 13 14 15 16
May-June 2000
July-Aug 2000
NEWPORT
HECETA HEAD
COOS BAY
CAPE BLANCO
CRESCENT CITY
OREGON
CALIFORNIA
5-m Salinity
30.0 30.4 30.8 31.2 31.6 32.0 32.4 32.8 33.2
Geopotential anomaly (m² s⁻²) at 5 m relative to 100 m
0.4 0.8 1.2 1.6 2.0 2.4 2.8 3.2 3.6
45
44
43
42
126 125 124 W
126 125 124 123 W

4. Discussion

We were able to explain a high percentage (up to 94%) of the variation in cetacean distribution using measured oceanographic data. Certainly, having fine-scale ocean and cetacean data on comparable space and time scales was important; however, even with fine-scale concurrent sampling of oceanographic variables and cetacean distribution, the high variance explained is most likely due to cetaceans knowing their environment and actively selecting habitat having certain measurable and consistent oceanographic qualities. Predator knowledge is recognized as a key component in the relationship between animal behavior and ocean structure (Matthiopoulos, 2003). With our GLOBEC surveys of the northern CCS, we were able to measure those important ocean features and upwelling structure quantitatively on similar space and time scales to the cetaceans. The merit of interdisciplinary approaches in cetacean research has been established through comparisons of cetacean distributions with hydrographic features (Smith et al., 1986; Tynan, 1997; Reilly, 1990; Davis et al., 2002; Jaquet and Gendron, 2002), as well as associations with prey (Schoenherr, 1991; Wishner et al., 1995; Croll et al., 1998; Fiedler et al., 1998; Tynan, 1998; Benson et al., 2002; Gill, 2002). However, the necessity in some studies to pool data into large $\geqslant 2^{\circ}$ latitude-longitude blocks can impose a minimum level of resolution in models (Jaquet et al., 1996; Reilly, 1990). Comparisons of mammal distributions with monthly mean indices of upwelling (Keiper et al., 2005) also can negate the importance of upwelling dynamics on finer temporal scales. In the present study, the synoptic, high resolution of the biophysical processes associated with upwelling and the circulation of the northern CCS provided a close spatial and temporal comparison with the cetacean survey data.

Flow-topography interactions between the northern California Current and Heceta Bank (ca. 44.0–44.5°N) strongly influenced cetacean distributions. The ADCP-derived current vectors suggest a recirculation over the bank, with southward flow over the northern and western regions of the bank and some eastward and northward flow at the southern edge. Humpback whales occurred on the bank during August, when their distribution was significantly correlated with high chlorophyll concentration and higher backscatter at 38 kHz (i.e. larger prey such as fish). The highest catch of juvenile chinook *Oncorhynchus tshawytscha* and coho salmon *O. kisutch* (10–25 fish per catch) (Brodeur et al., 2004), as well as the highest abundance of Pacific sardine *Sardinops sagax* (1000–10,000 fish per catch; R.D. Brodeur, unpublished data NMFS) occurred where humpbacks concentrated on Heceta Bank. During August, the highest densities and largest daytime patches of euphausiids $\geqslant 10$ mm in length (dominated by *E. pacifica*) also occurred over Heceta Bank (Ressler et al., 2005).

Therefore, it appears that by August, humpback whales were responding to a cascade of trophic dynamics enhanced by the flow-topography interactions and the broad upwelling signature over the bank. The extraordinary success of our multiple logistic regression model to explain variance in humpback occurrence during August (94.4%), is likely due to the success of the models to capture the occurrence of humpbacks near these 'hot spots' of increased prey density.

Although Heceta Bank is among the largest submarine banks on the west coast (Hickey, 1998),

Fig. 7. The correspondence of sightings of Pacific white-sided dolphins (○) and Dall's porpoises (*) with sea surface (5 m) temperature, surface salinity, and geopotential anomaly at 5 m relative to 100 m, during May–June and July–August 2000. Several features related to upwelling were included in the models of cetacean occurrence: the center of the equatorward jet, defined by geopotential anomaly $2.35\,m^2\,s^{-2}$ (the double heavy line); the shoreward edge of the jet, defined by geopotential anomaly $2.0\,m^2\,s^{-2}$ (first single heavy line inshore of the jet center); and the shoreward edge of the surface front in SST, defined by the 11.5 °C isotherm (blue-to-green boundary) during June, and the 12.0 °C isotherm during August. The symbols mark the location of sightings and do not reflect the number of dolphins or porpoises in each sighting. The occurrence of Pacific white-sided dolphins in or west of the center of the jet, in warmer, lower salinity surface water, is evident during June. During August, the occurrence of Dall's porpoise between the center and shoreward edge of the jet and upwelling front is clear.

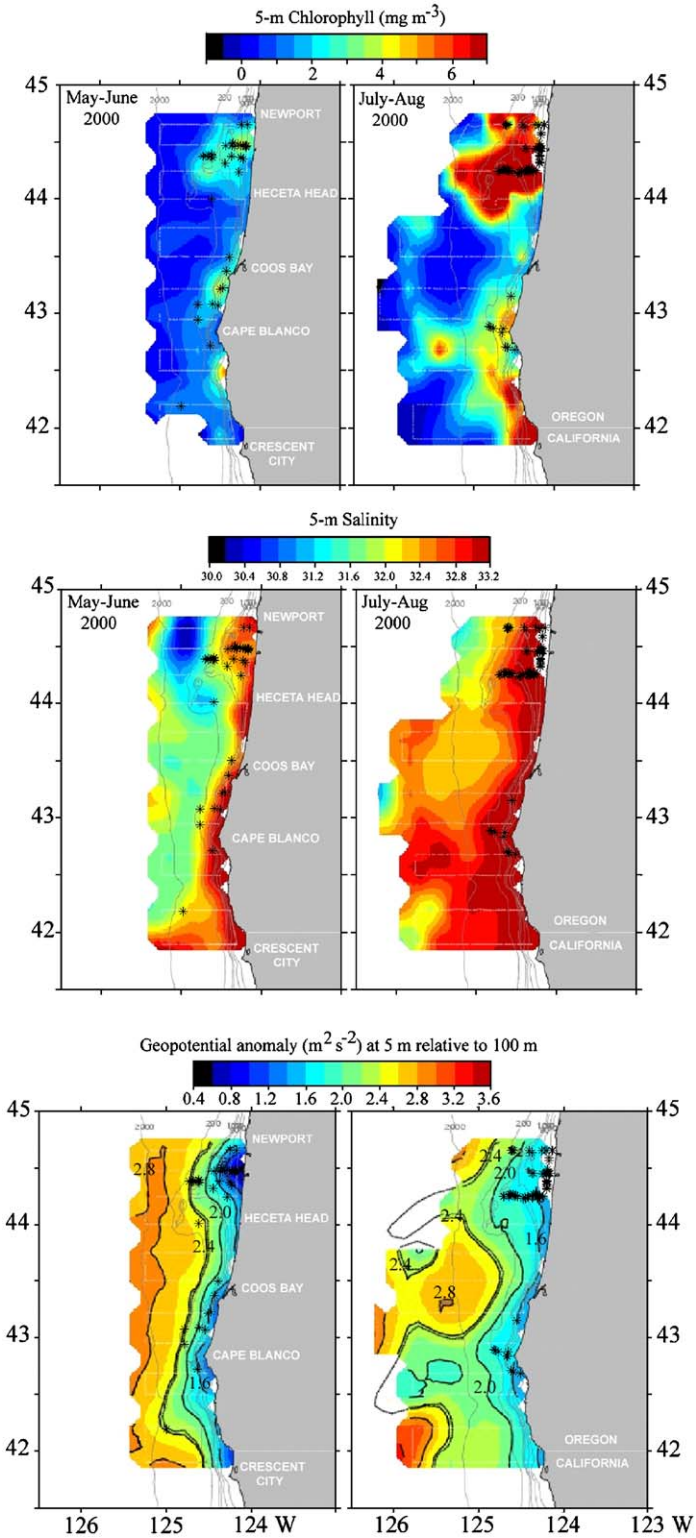
5-m Chlorophyll (mg m-3)
0 2 4 6
May-June 2000
July-Aug 2000
NEWPORT
HECETA HEAD
COOS BAY
CAPE BLANCO
CRESCENT CITY
OREGON
CALIFORNIA
5-m Salinity
30.0 30.4 30.8 31.2 31.6 32.0 32.4 32.8 33.2
Geopotential anomaly (m2 s-2) at 5 m relative to 100 m
0.4 0.8 1.2 1.6 2.0 2.4 2.8 3.2 3.6
45
44
43
42
126 125 124 W
126 125 124 123 W

internal hydraulic flows associated with even smaller features on this bank (i.e. Stonewall Bank) can greatly enhance turbulence in the bottom boundary layer (Nash and Moum, 2001). Fine-scale process studies to examine associations between foraging cetaceans, their prey and the circulation of banks warrants further study. In the southeast Bering Sea, foraging whales occur on the middle shelf (50–100 m) where the mean currents are sluggish, but tidal currents are energetic (Tynan, 2004). Here, we hypothesize that the enhanced vertical and horizontal mixing associated with Heceta Bank is linked to higher prey densities and hence, improved foraging for cetaceans, especially humpback whales and harbor porpoises. During August, humpback whales were observed feeding along and near a series of parallel alongshore fronts on Heceta Bank. The fronts may have resulted from internal wave field passage.

The surveys during June and August 2000 provided an opportunity to compare the seasonal shift in the position of the equatorward coastal jet with the distribution of cetaceans. Typically, the jet forms near the coast during spring upwelling and moves offshore with sustained upwelling (Moum and Nash, 2000). The longitudinal position of the shoreward edge of the surface front however is not greatly different between June and August 2000, although during August the mesoscale structure was enhanced and the surface front was especially convoluted on Heceta Bank. In addition, the intrusion of a warm low-chlorophyll mesoscale meander offshore (ca. 43–44°N) during August restricted the offshore movement of upwelled waters and compressed the system to the north, south and east. This feature also may have compressed distributions of slope-inhabiting cetaceans, such as Dall's porpoise, to the periphery of the meander between the center and shoreward edge of the equatorward jet. The increased mesoscale variability during summer in this way improved the percentage of explained variance in Dall's porpoise occurrence pattern. Shoaling isopycnals at the edge of the meander may also have compressed the depth range of their fish or cephalopod prey (Walker, 1996), thereby enhancing foraging at the periphery.

Pacific white-sided dolphin, which was the dominant small cetacean over the slope in June, was very rare in the system during August; however, their high seasonality likely reflects a movement or migration from the region more than a regional displacement by the warm mesoscale meander in August. The strong correlation between Pacific white-sided dolphins and backscatter at 38 kHz suggests that during spring they were following mesopelagic fish, although cephalopods are also important in the diet (Walker and Jones, 1990).

The distributions of harbor porpoises and humpback whales were significantly associated with the position of the alongshore upwelling front in both seasons; however more humpback whales occurred offshore on the western edge of the jet and upwelling front in June. In contrast, by August, humpback whales and harbor porpoises concentrated in high-chlorophyll shelf waters on the inshore side of the jet and surface front at Heceta Bank and near Cape Blanco. The region inshore of the surface front is associated with convergence (i.e. cross-shelf streamlines leave the surface shoreward of the density front; Allen et al., 1995, their Figs. 4 and 5), and therefore, with the potential concentration of prey. The flow-topography interactions that contribute to the positions of the jet and the inshore edge of the upwelling front are here recognized as key

Fig. 8. The correspondence of sightings of harbor porpoises (*) with surface (5 m) chlorophyll, surface salinity, and geopotential anomaly at 5 m relative to 100 m, during May–June and July–August 2000. Several features related to upwelling were included in the models of cetacean occurrence: the center of the equatorward jet, defined by geopotential anomaly 2.35 $m^2 s^{-2}$ (the double heavy line); the shoreward edge of the jet, defined by geopotential anomaly 2.0 $m^2 s^{-2}$ (first single heavy line inshore of the jet center); and the shoreward edge of the surface front in SST, defined by the 11.5 °C isotherm (blue-to-green boundary) during June and the 12.0 °C isotherm during August. During June, harbor porpoise occurrence is restricted to the shelf, near the upwelling front and shoreward of the center of the jet. The high density of harbor porpoise in upwelled waters on Heceta Bank during August corresponds with the shoreward edge of the surface front, high surface chlorophyll, and high salinity.

processes to include in predictive models of cetacean occurrence in the CCS. Similar processes and features may also be important in determining cetacean distributions in other boundary current systems of the world.

Humpback whales arrive in the northern CCS in spring after spending the winter off Mexico (Calambokidis et al., 2000). During spring, humpback whale occurrence was significantly correlated with the warmer SSTs over the slope; however, since some humpbacks occurred in the cold recently upwelled water of higher backscatter at 38 kHz (i.e. likely fish), it is assumed that humpbacks can tolerate the cold (~9 °C) conditions after they arrive. Humpbacks did appear to avoid the lowest salinity water of Columbia River origin; however, they occurred at the salinity front associated with the offshore plume. During spring, humpbacks off and south of Cape Blanco were significantly correlated with the center of the equatorward jet. Our models demonstrate the important predictive capacity of dynamic height; it is encouraging that this variable could be applied in models of occurrence in other boundary current systems.

Both slope-associated Dall's porpoise and shelf-associated harbor porpoise were significantly associated with integrated backscatter at 420 kHz during spring. For both species, backscatter at 420 kHz was the most important predictive biological variable during June. It is possible that backscatter of zooplankton at the high frequencies serves as a better proxy for the porpoises' prey (i.e. fish and cephalopods), especially for species that may diurnally migrate from depths below 100 m (or deeper than the depth integration of acoustic backscatter, 0–100 m). However, though it is tempting to assume that backscatter at 420 kHz is indicative of copepods, an important caveat in the interpretation of integrated backscatter is that high abundances of gelatinous zooplankton can contribute significantly to backscatter measured at $\geqslant$200 kHz (Monger et al., 1998). Therefore, interpretation of the associations between cetaceans and backscatter at higher frequencies (i.e. 200 or 420 kHz) awaits further resolution of the bioacoustic data to more specific taxonomic definition using net collections.

The presence of sperm whales in slope waters off Heceta Bank in spring and summer suggests that their cephalopod or fish prey are predictably abundant over the steep and rough topography in this region. In general, large cephalopods and fish are the primary and secondary prey, respectively, of sperm whales off California (Kawakami, 1980). There, the large squid *Moroteuthis robusta* is an important prey species of sperm whales (Fiscus et al., 1989); specimens of $>$1 m lengths have been caught off Oregon in water deeper than 150 m (Pearcy, 1965). Though squid were not specifically studied during GLOBEC, some earlier studies suggest that an influx or migration of squid into slope waters off Oregon occurs during summer (Pearcy, 1965).

The association of sperm whales and beaked whales (i.e. *B. bairdii*, *Z. cavirostris*, and *Mesoplodon* sp.) with a dynamic region of surface convergence between the southward flowing jet and the northward flow along the edge of an anticyclonic mesoscale eddy during August suggests that flow-topography interactions along the slope near Heceta Bank are important to large odontocetes and their prey. We hypothesize that strong turbulence associated with rough topography (Kunze and Toole, 1997) and interactions of the internal tide with a critical slope (Thorpe et al., 1990; Moum et al., 2002) may influence foraging sperm whales and beaked whales through linkages between their cephalopod or fish prey and enhanced nepheloid layers at regions of high mixing over the continental slope.

Acknowledgements

The captains and crews of the R.V. *New Horizon* and R.V. *Wecoma* were very helpful in the successful completion of the cetacean surveys and the operation of the towed vehicle SeaSoar, respectively. The expertise and dedication of the cetacean observers, M. Force, G. Krutzikowsky, K. Maze, M. Newcomer, and T. Pusser were invaluable to the quality of the sightings data. We thank R. O'Malley for help in collecting and processing the SeaSoar hydrographic data and for calculating the SeaSoar-derived environmental

indices used in this analysis. We also thank OSU Marine Technicians, M. Willis, L. Fayler, D. Swensen and T. Martin for helping us to collect high-quality data from SeaSoar. The officers and crew of the R.V. *Wecoma* did an outstanding job towing along our mapping grids while avoiding fishing boat traffic and fixed fishing gear. This research, conducted as part of US GLOBEC Northeast Pacific Program, was jointly funded by the National Science Foundation and NOAA Coastal Ocean Program (COP), with support to CTT for analyses provided by NOAA COP, through a Woods Hole Oceanographic Institution-CICOR grant NA17RJ1223, and Office of Naval Research Grant N00014-03-1-0330. Operational, logistical, and administrative support was provided by the Northwest Fisheries Science Center – NOAA, Oregon State University and NOAA's Hatfield Marine Science Center and the Woods Hole Oceanographic Institution, where as such this manuscript represents WHOI Contribution Number 11035. This is contribution number 483 of the US GLOBEC program. We dedicate this research in memory of Michael W. Newcomer, who so enjoyed spending a beautiful day surveying cetaceans and seabirds, always wondering what might be just over the horizon.

References

Ainley, D.G., Boekelheide, R.J. (Eds.), 1990, Seabirds of the Farallon Islands: Ecology, Structure and Dynamics of an Upwelling System Community. Stanford University Press, Palo Alto (425pp).

Ainley, D.G., Spear, L.B., Allen, S.G., 1996. Variation in the diet of Cassin's auklet reveals spatial, seasonal, and decadal occurrence patterns of euphausiids off California, USA. Marine Ecology Progress Series 137, 1–10.

Ainley, D.G., Spear, L.B., Tynan, C.T., Barth, J.A., Pierce, S.D., Ford, R.G., Cowles, T.J., 2005. Physical and biological variables affecting seabird distributions during the upwelling season of the northern California Current. Deep-Sea Research II, this issue [doi:10.1016/j.dsr2.2004.08.016].

Allen, J.S., Newberger, P.A., Federiuk, J., 1995. Upwelling circulation in shore on the Oregon continental shelf. Part I: response to idealized forcing. Journal of Physical Oceanography 25, 1843–1866.

Barth, J.A., Pierce, S.D., Smith, R.L., 2000. A separating coastal upwelling jet at Cape Blanco, Oregon and its connection to the California Current System. Deep-Sea Research II 47, 783–810.

Barth, J.A., Cowles, T.J., Kosro, P.M., Shearman, R.K., Huyer, A., Smith, R.L., 2002. Injection of carbon from the shelf to offshore beneath the euphotic zone in the California Current. Journal of Geophysical Research 107 (6), 3057.

Barth, J.A., Pierce, S.D., Cowles, T.J., 2005. Mesoscale structure and its seasonal evolution in the northern California Current System. Deep-Sea Research II, this issue [doi:10.1016/j.dsr2.2004.09.026].

Batchelder, H.P., Barth, J.A., Kosro, P.M., Strub, P.T., Brodeur, R.D., Peterson, W.T., Tynan, C.T., Ohman, M.D., Botsford, L.W., Powell, T.M., Schwing, F.B., Ainley, D.G., Mackas, D.L., Hickey, B.M., Ramp, S.R., 2002. The GLOBEC Northeast Pacific California Current System Program. Oceanography 15, 36–47.

Batteen, M.L., 1997. Wind-forcing modeling studies of currents, meanders and eddies in the California Current System. Journal of Geophysical Research 102, 985–1010.

Benson, S.R., Croll, D.A., Marinovic, B.B., Chavez, F.P., Harvey, J.T., 2002. Changes in the cetacean assemblage of a coastal upwelling ecosystem during El Niño 1997–98 and La Niña 1999. Progress in Oceanography 54, 279–291.

Brodeur, R.D., Pearcy, W.G., 1992. Effects of environmental variability on trophic interactions and food web structure in a pelagic upwelling ecosystem. Marine Ecology Progress Series 84, 101–119.

Brodeur, R.D., Fisher, J.P., Teel, D., Emmett, R.L., Casillas, E., Miller, T.W., 2004. Juvenile salmonid distribution, growth, condition, origin, environmental and species associations in the Northern California Current. Fishery Bulletin US 102, 25–46.

Calambokidis, J., et al., 2000. Migratory destinations of humpback whales that feed off California, Oregon and Washington. Marine Ecology Progress Series 192, 295–304.

Cox, D.R., Snell, E.J., 1989. Analysis of Binary Data. Chapman & Hall, London.

Croll, D.A., Tershy, B.R., Hewitt, R.P., Demer, D.A., Fiedler, P.C., Smith, S.E., Armstrong, W., Popp, J.M., Kiekhefer, T., Lopez, V.R., Urban, J., Gendron, D., 1998. An integrated approach to the foraging ecology of marine birds and mammals. Deep-Sea Research II 45, 1353–1371.

Davis, R.W., Ortega-Ortiz, J.G., Ribic, C.A., Evans, W.E., Biggs, D.C., Ressler, P.H., Cady, R.B., Leben, R.R., Mullin, K.D., Würsig, B., 2002. Cetacean habitat in the northern oceanic Gulf of Mexico. Deep-Sea Research I 49, 121–142.

Fiedler, P.C., Reilly, S.B., Hewitt, R.P., Demer, D., Philbrick, V.A., Smith, S., Armstrong, W., Croll, D.A., Tershy, B.R., Mate, B.R., 1998. Blue whale habitat and prey in the California Channel Islands. Deep-Sea Research II 45, 1781–1801.

Fiscus, C.H., Rice, D.W., Wolman, A.A., 1989. Cephalopods from the stomachs of sperm whales taken off California. NOAA Technical Report NMFS 83 (12pp).

Gill, P.G., 2002. A blue whale (*Balaenoptera musculus*) feeding ground in a southern Australian coastal upwelling zone. The Journal of Cetacean Research and Management 4 (2), 179–184.

Hickey, B.M., 1998. Coastal oceanography of western North America from the tip of Baja California to Vancouver Island. In: Robinson, A.R., Brink, K.H. (Eds.), The Global Coastal Ocean. The Sea, vol. 11. John Wiley & Sons, Inc., New York, pp. 345–393.

Hood, R.R., Abbott, M.R., Huyer, A., Kosro, P.M., 1990. Surface patterns in temperature, flow, phytoplankton biomass, and species composition in the coastal transition zone off northern California. Journal of Geophysical Research 95, 18081–18094.

Huyer, A., Smith, R.L., 1974. A subsurface ribbon of cold water over the continental shelf off Oregon. Journal of Physical Oceanography 4, 381–391.

Jaquet, N., Gendron, D., 2002. Distribution and relative abundance of sperm whales in relation to key environmental features, squid landings and the distribution of other cetacean species in the Gulf of California, Mexico. Marine Biology 141, 591–601.

Jaquet, N., Whitehead, H., Lewis, M., 1996. Coherence between 19th century sperm whale distributions and satellite-derived pigments in the tropical Pacific. Marine Ecology Progress Series 145, 1–10.

Kawakami, T., 1980. A review of sperm whale food. The Scientific Reports of the Whales Research Institute 32, 199–218.

Keiper, C.A., Ainley, D.G., Allen, S.G., Harvey, J.T., 2005. Inter-annual variability in patterns of marine mammal occurrence and ocean climate off central California, 1986–1994, 1997–1999. Marine Ecology Progress Series, in press.

Kleinbaum, D.G., Kupper, L.L., Muller, K.E., 1988. Applied Regression Analysis and Other Multivariate Methods. PWS-KENT Publishing Company, Boston.

Kundu, P.K., Allen, J.S., 1976. Some three-dimensional characteristics of low-frequency current fluctuations near the Oregon coast. Journal of Physical Oceanography 6, 181–199.

Kunze, E., Toole, J.M., 1997. Tidally driven vorticity, diurnal shear and turbulence atop Fieberling Seamount. Journal of Physical Oceanography 27, 2663–2693.

Mantua, N.J., Hare, S.R., Zhang, Y., Wallace, J.M., Francis, R.C., 1997. A Pacific interdecadal climate oscillation with impacts on salmon production. Bulletin of the American Meteorological Society 78, 1069–1079.

Matthiopoulos, J., 2003. The use of space by animals as a function of accessibility and preference. Ecological Modeling 159, 239–268.

Monger, B.C., Chinniah-Chandy, S., Meir, E., Billings, S., Greene, C.H., Wiebe, P.H., 1998. Sound scattering by the gelatinous zooplankters *Aequorea victoria* and *Pleurobrachia bachei*. Deep-Sea Research II 45, 1255–1271.

Moum, J.N., Nash, J.D., 2000. Topographically induced drag and mixing at a small bank on the continental shelf. Journal of Physical Oceanography 30, 2049–2054.

Moum, J.N., Caldwell, D.R., Nash, J.D., Gunderson, G.D., 2002. Observations of boundary mixing over the continental slope. Journal of Physical Oceanography 32, 2113–2130.

Nash, J.D., Moum, J.N., 2001. Internal hydraulic flows on the continental shelf: high drag states over a small bank. Journal of Geophysical Research 106, 4593–4611.

Pearcy, W.G., 1965. Species composition and distribution of pelagic cephalopods from the Pacific Ocean off Oregon. Pacific Science 19, 261–266.

Peterson, W.T., Schwing, F.B., 2003. A new climate regime in Northeast Pacific ecosystems. Geophysical Research Letters 30 (17), 1896.

Pollard, R., 1986. Frontal surveys with a towed profiling conductivity/temperature/depth measurement package (SeaSoar). Nature 323, 433–435.

Reid, J.L., Mantyla, A.W., 1976. The effect of geostrophic flow upon coastal sea elevations in the northern North Pacific Ocean. Journal of Geophysical Research 81, 3100–3110.

Reilly, S.B., 1990. Seasonal changes in distribution and habitat differences among dolphins in the eastern tropical Pacific. Marine Ecology Progress Series 66, 1–11.

Ressler, P.H., Brodeur, R.D., Peterson, W.T., Pierce, S.D., Vance, P.M., Røstad, A., Barth, J.A., 2005. The spatial distribution of euphausiid aggregations in the northern California Current during August 2000. Deep-Sea Research II, this issue [doi:10.1016/j.dsr2.2004.09.032].

Roemmich, D., McGowan, J., 1995. Climate warming and the decline of zooplankton in the California Current. Science 267, 1324–1326.

Schoenherr, J.R., 1991. Blue whale feeding on high concentrations of euphausiids around Monterey submarine canyon. Canadian Journal of Zoology 69, 583–594.

Seber, G.A.F., 1977. Linear Regression Analysis. John Wiley & Sons, Inc., New York.

Smith, R.C., Dustan, P., Au, D., Baker, K.S., Dunlap, E.A., 1986. Distributions of cetaceans and sea surface chlorophyll concentrations in the California Current. Marine Biology 91, 385–402.

Smith, R.L., Huyer, A., Kosro, P.M., Barth, J.A., 1999. Observations of El Niño off Oregon: July 1997 to present (October 1998). PICES Scientific Report, No. 10, pp. 33–37.

S-PLUS, 1997. S-PLUS 4 Guide to Statistics. Data Analysis Products Division, MathSoft, Seattle.

StataCorp, 1995. Stata Reference Manual: Release 5.1, sixth ed., College Station, Texas, Stata Corporation.

Strub, P.T., Allen, J.S., Huyer, A., Smith, R.L., 1987. Seasonal cycles of currents, temperatures, winds, and sea level over the northeast Pacific continental shelf: 35N to 48N. Journal of Geophysical Research 92, 1507–1526.

Strub, P.T., Kosro, P.M., Huyer, A., CTZ Collaborators, 1991. The nature of the cold filaments in the California Current system. Journal of Geophysical Research 96, 14743–14768.

Strub, P.T., Batchelder, H.P., Weingartner, T.J., 2002. US GLOBEC Northeast Pacific program: overview. Oceanography 15, 30–47.

Thorpe, S.A., Hall, P., White, M., 1990. The variability of mixing at the continental slope. Proceedings of the Royal

Society of London, Series A: Mathematics and Physical Sciences A331, 183–194.

Tynan, C.T., 1997. Cetacean distributions and oceanographic features near the Kerguelen Plateau. Geophysical Research Letters 24, 2793–2796.

Tynan, C.T., 1998. Ecological importance of the Southern Boundary of the Antarctic Circumpolar Current. Nature 392, 708–710.

Tynan, C.T., 2004. Cetacean populations on the southeastern Bering Sea shelf during the late 1990s: implications for decadal changes in ecosystem structure and carbon flow. Marine Ecology Progress Series 272, 281–300.

Walker, W.A., 1996. Summer feeding habits of Dall's porpoise, *Phocoenoides dalli*, in the southern Sea of Okhotsk. Marine Mammal Science 12, 167–181.

Walker, W.A., Jones, L.L., 1990. Food habits of northern right whale dolphin, Pacific white-sided dolphin, and northern fur seal caught in the high seas driftnet fisheries of the North Pacific Ocean, 1990. Bulletin International North Pacific Fisheries Commission 53, 285–295.

Wishner, K.F., Schoenherr, J.R., Beardsley, R., Chen, C., 1995. Abundance, distribution and population structure of the copepod *Calanus finmarchicus* in a springtime right whale feeding area in the southwestern Gulf of Maine. Continental Shelf Research 15, 475–507.